



Stimulation of frontal pathways disrupts hand muscle control during object manipulation

Luca Viganò,^{1,†} Henrietta Howells,^{2,†} Marco Rossi,¹ Marco Rabuffetti,³ Guglielmo Puglisi,^{1,2} Antonella Leonetti,¹ Andrea Bellacicca,² Marco Conti Nibali,¹ Lorenzo Gay,¹ Tommaso Sciortino,¹ Gabriella Cerri,² Lorenzo Bello¹ and Luca Forna²

[†]These authors contributed equally to this work.

The activity of frontal motor areas during hand-object interaction is coordinated by dense communication along specific white matter pathways. This architecture allows the continuous shaping of voluntary motor output but, despite extensive investigation in non-human primate studies, remains poorly understood in humans. Disclosure of this system is crucial for predicting and treatment of motor deficits after brain lesions.

For this purpose, we investigated the effect of direct electrical stimulation on white matter pathways within the frontal lobe on hand-object manipulation. This was tested in 34 patients (15 left hemisphere, mean age 42 years, 17 male, 15 with tractography) undergoing awake neurosurgery for frontal lobe tumour removal with the aid of the brain mapping technique. The stimulation outcome was quantified based on hand-muscle activity required by task execution. The white matter pathways responsive to stimulation with an interference on muscles were identified by means of probabilistic density estimation of stimulated sites, tract-based lesion-symptom (disconnectome) analysis and diffusion tractography on the single patient level. Finally, we assessed the effect of permanent tract disconnection on motor outcome in the immediate postoperative period using a multivariate lesion-symptom mapping approach.

The analysis showed that stimulation disrupted hand-muscle activity during task execution at 66 sites within the white matter below dorsal and ventral premotor regions. Two different EMG interference patterns associated with different structural architectures emerged: (i) an ‘arrest’ pattern, characterized by complete impairment of muscle activity associated with an abrupt task interruption, occurred when stimulating a white matter area below the dorsal premotor region. Local middle U-shaped fibres, superior fronto-striatal, corticospinal and dorsal fronto-parietal fibres intersected with this region; and (ii) a ‘clumsy’ pattern, characterized by partial disruption of muscle activity associated with movement slowdown and/or uncoordinated finger movements, occurred when stimulating a white matter area below the ventral premotor region. Ventral fronto-parietal and inferior fronto-striatal tracts intersected with this region. Finally, only resections partially including the dorsal white matter region surrounding the supplementary motor area were associated with transient upper-limb deficit ($P = 0.05$; 5000 permutations).

Overall, the results identify two distinct frontal white matter regions possibly mediating different aspects of hand-object interaction via distinct sets of structural connectivity. We suggest the dorsal region, associated with arrest pattern and postoperative immediate motor deficits, to be functionally proximal to motor output implementation, while the ventral region may be involved in sensorimotor integration required for task execution.

Received June 07, 2021. Revised August 20, 2021. Accepted September 15, 2021. Advance access publication October 8, 2021

© The Author(s) (2021). Published by Oxford University Press on behalf of the Guarantors of Brain.

This is an Open Access article distributed under the terms of the Creative Commons Attribution-NonCommercial License (<https://creativecommons.org/licenses/by-nc/4.0/>), which permits non-commercial re-use, distribution, and reproduction in any medium, provided the original work is properly cited. For commercial re-use, please contact journals.permissions@oup.com

- 1 Neurosurgical Oncology Unit, Department of Oncology and Hemato-Oncology, Università degli Studi di Milano, Milano, Italy
- 2 MoCA Laboratory, Department of Medical Biotechnology and Translational Medicine, Università degli Studi di Milano, Milano, Italy
- 3 IRCCS Fondazione Don Carlo Gnocchi, Milano, Italy

Correspondence to: Gabriella Cerri
 Department of Medical Biotechnology and Translational Medicine
 Università degli Studi di Milano, Via Fratelli Cervi
 E-mail: gabriella.cerri@unimi.it

Keywords: intraoperative brain mapping; EMG; object manipulation; diffusion tractography; hand motor control

Abbreviations: aCC = autocorrelation coefficient; CST = corticospinal tract; DES = direct electrical stimulation; HMT = hand-object manipulation task; FST = fronto-striatal tract; M1 = primary motor cortex; Mid-U = middle U-shaped fibres; PDE = probability density estimation; SLF = superior longitudinal fasciculus; PM = premotor area; SMA = supplementary motor area; SVR-LSM = support vector regression lesion symptom mapping

Introduction

The ability to manipulate objects is a key behaviour that allows humans to interact with their environment. Humans have particularly refined dexterity over other non-human primates, due to the unique structure of their hands¹ and the high density of direct projections from the primary motor cortex (M1) to spinal motoneurons.² To generate the adequate descending motor command, premotor areas and direct-indirect cortico-thalamic loops act in parallel to refine multiple aspects, from movement planning, selection, sequencing and inhibition to sensorimotor transformations and on-line updating of the motor program.^{3–8} The orchestrated activity of these networks is supported by specific white matter projections.^{9–14} In humans, these pathways have been anatomically described¹⁵; however, their role in controlling hand muscles during object manipulation has never been directly tested by means of an invasive electrophysiological approach. A comprehensive description of the connective anatomy of motor control is still lacking in comparative functional neuroanatomy¹⁶ but seems crucial for clinical practice from surgical interventions to neurorehabilitation.^{17,18}

To this aim, the integration between intraoperative direct electrical stimulation (DES), with its direct access to the functional role of white matter sites during brain mapping,^{19–21} and diffusion tractography, which can model white matter connections, represents one of the most promising approaches in humans. Recent developments in diffusion tractography enables the investigation of white matter pathways at high resolution²² and the visualization of fronto-parietal fibres crucial for motor control.^{23,24} In cases where tractography has not been performed, tract-based lesion-symptom analysis using the ‘disconnectome’ approach generates probabilistic maps of connections from a given region of interest, such as a functionally eloquent stimulation site, enabling the consideration of a stimulation effect as the result of a disconnection within a wider network.^{9,25}

In the context of intraoperative brain mapping for tumour removal, we recently demonstrated that stimulation of distinct precentral cortical sectors during the execution of an haptically-driven hand-object manipulation task (HMT) interferes with muscle activity with distinguishing features. This suggested that DES, applied while performing a specific hand motor task coupled with electromyographic recording, may reveal areas mediating different aspects of motor control possibly via distinct networks.^{26–29}

Within the same clinical context and with the same stimulation paradigm, we here investigate the anatomo-functional organization of white matter below premotor areas during the same task. To this aim, we assessed whether subcortical DES caused interferences in hand muscle patterns during the HMT in 36 patients undergoing awake surgery for removal of a brain tumour. Quantitative analysis of muscle activity affected at eloquent sites and their anatomical distribution were assessed using a spatial probability methodology developed in previous studies.^{21,26,28} We evaluated the affected white matter tracts for each patient by using a disconnectome approach²⁵ for different stimulation effects based on high angular resolution diffusion imaging tractography of healthy subjects acquired by the Human Connectome Project (7 T protocol). We refined this result in a subset of 15 patients that underwent preoperative diffusion tractography, using their unique intraoperative stimulation site and white matter tractogram. Finally, to investigate whether postoperative motor deficits were associated with resection of a specific white matter region, we performed support vector regression lesion-symptom mapping (SVR-LSM) using patients’ postoperative resection cavities ($n = 34$). In the subset of patients with diffusion tractography ($n = 15$), the postoperative motor outcome was correlated with the percentage of disconnection for different white matter tracts. This is a novel study combining electrophysiological and structural neuroimaging to directly investigate frontal white matter recruited during object manipulation. A flowchart of the methods adopted in the study is shown in Fig. 1. The results are discussed in light of hodological and electrophysiological evidence in non-human primate investigating hand-related pathways. A more thorough appreciation of the anatomo-functional organization and functional properties of this network is crucial for a safe and effective resection of tumours involving this area.

Materials and methods

Study design and patient cohort

Thirty-four patients that were candidates for an awake neurosurgical resection for a left ($n = 15$) or right ($n = 19$) hemisphere brain tumour at the Surgical Neuro-oncology Unit (of L.B.) between 2016 and 2019 (Table 1) were studied. All participants gave written informed consent to the surgical mapping procedure (IRB1299) and

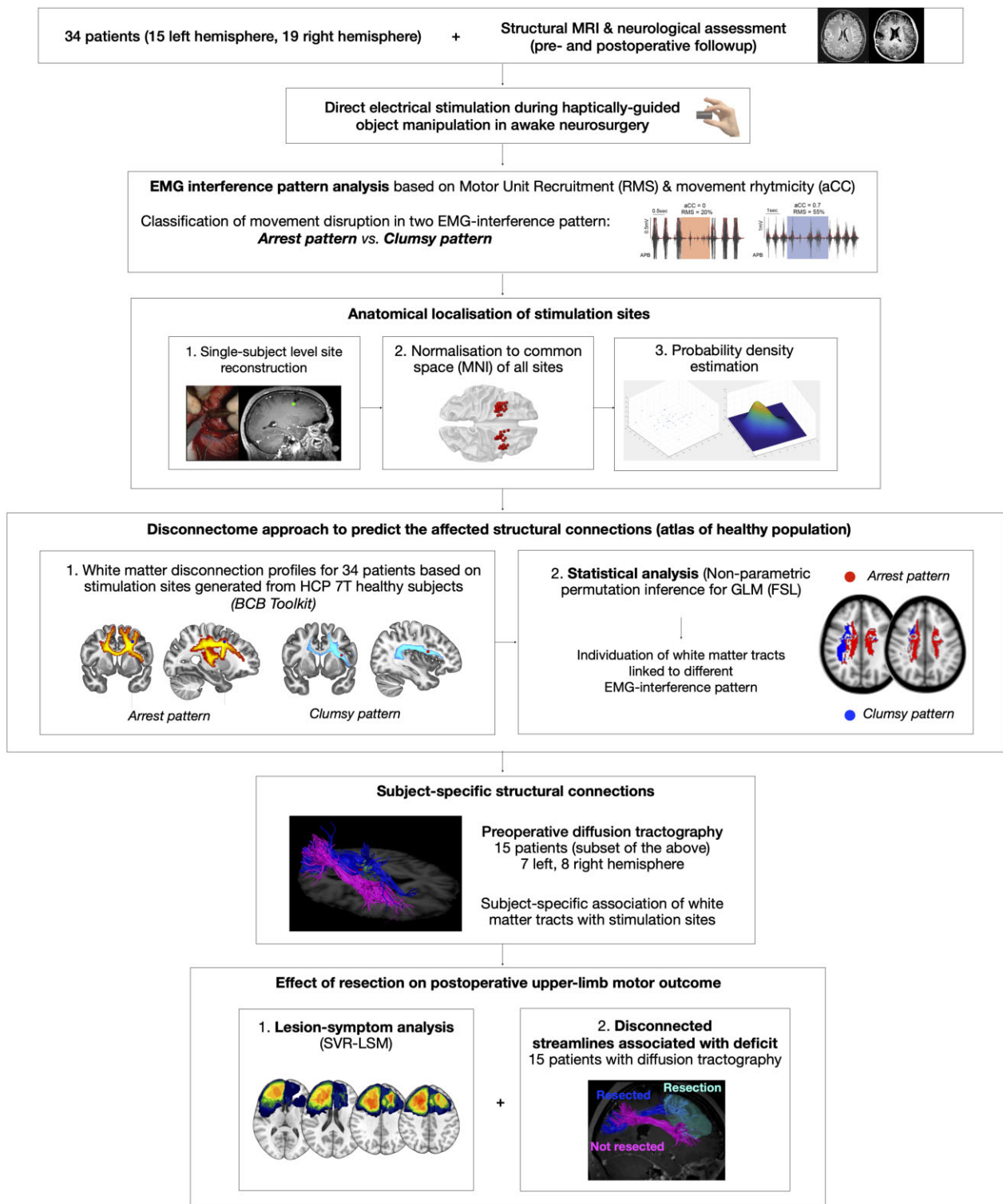


Figure 1 Study flow chart.

data analysis for research purposes, following the principles outlined in the Declaration of Helsinki. The study was performed with strict adherence to the clinical procedure for tumour removal. Patients were included if they fulfilled the following criteria: no preoperative motor deficits, no long-term history of epilepsy and no previous neurosurgical needle or open biopsy, no tumour infiltration of the tested area. All

patients were assessed for handedness using the Edinburgh Handedness Inventory and underwent a preoperative, 5-day and 1-month postoperative neuropsychological evaluation of cognitive ability and neurological examinations of motor ability.³⁰ Surgical resection was aimed at supratotal resection,³¹ involving at the posterior border of the resection cavity the connectivity in the tested area.

Table 1 Demographic and clinical information about the entire sample

Patient no	Hem	Histology	Grade	Eor	Sex	Age	Handedness	5-Day MRC scale	De Renzi score
1	Right	Astrocytoma	III	Supratotal	Male	43	Right	2 (SMA syndrome)	n.a.
2	Right	Anaplastic astrocytoma	III	Supratotal	Male	59	Right	5	3
3	Right	Oligodendroglioma	II	Supratotal	Male	29	Right	5	3
4	Left	Glioblastoma	IV	Total	Female	64	Right	5	3
5	Left	Anaplastic oligodendroglioma	III	Supratotal	Female	46	Right	5	3
6	Right	Astrocytoma	II	Supratotal	Male	27	Right	5	3
7	Left	Oligodendroglioma	III	Total	Male	45	Right	5	3
8	Right	Astrocytoma	II	Supratotal	Female	35	Right	5	3
9	Left	Oligodendroglioma	II	Supratotal	Female	38	Right	5	2
10	Right	Anaplastic oligodendroglioma	III	Total	Female	54	Right	5	3
11	Left	Glioblastoma	IV	Total	Male	54	Right	5	3
12	Left	Glioblastoma	IV	Total	Male	38	Right	3	n.a.
13	Left	Neurocytoma	II	Total	Male	38	Right	2 (SMA syndrome)	n.a.
14	Right	Oligoastrocytoma	II	Supratotal	Female	22	Right	2 (SMA syndrome)	3
15	Right	Anaplastic astrocytoma	III	Supratotal	Male	38	Right	5	3
16	Left	Oligodendroglioma	II	Supratotal	Male	38	Right	5	3
17	Right	Glioblastoma	IV	Total	Female	39	Right	2	n.a.
18	Right	Oligodendroglioma	II	Supratotal	Female	22	Right	3	n.a.
19	Right	Oligodendroglioma	II	Supratotal	Female	34	Right	2 (SMA syndrome)	n.a.
20 ^a	Right	Astrocytoma	II	Total	Female	42	Right	3	n.a.
21 ^a	Left	Oligodendroglioma	II	Total	Male	41	Left	5	3
22 ^a	Left	Oligodendroglioma	III	Supratotal	Female	55	Right	5	3
23 ^a	Right	Oligodendroglioma	II	Supratotal	Male	31	Right	5	3
24 ^a	Right	Anaplastic astrocytoma	III	Supratotal	Male	28	Left	5	2
25 ^a	Right	Oligoastrocytoma	III	Supratotal	Female	49	Right	2	n.a.
26 ^a	Left	Astrocytoma	III	Supratotal	Female	40	Right	5	3
27 ^a	Right	Oligodendroglioma	II	Supratotal	Male	45	Left	5	3
28 ^a	Right	Astrocytoma	II	Supratotal	Female	29	Right	5	3
29 ^a	Left	Glioblastoma	IV	Supratotal	Female	34	Left	5	3
30 ^a	Right	Anaplastic astrocytoma	III	Total	Female	53	Right	5	3
31 ^a	Left	Astrocytoma	II	Supratotal	Female	57	Right	2	n.a.
32 ^a	Left	Glioblastoma	IV	Total	Male	54	Right	5	3
33 ^a	Left	Anaplastic astrocytoma	III	Supratotal	Male	40	Right	5	3
34 ^a	Right	Astrocytoma	II	Supratotal	Male	47	Right	5	3

De Renzi score: 3 (>62); 2 (53–62); 1 (<53); n.a. = not administrated. Eor = extent of resection; Hem = hemisphere.

^aPatients that underwent diffusion MRI for tractography.

Intraoperative subcortical brain mapping for object manipulation

Surgery was performed using asleep-awake-asleep anaesthesia, with the aim to identify pure motor (fibres originating from M1), praxis (see below), language, visual and cognitive boundaries.^{21,32–34} For praxis mapping during tumour resection, low frequency DES delivered by a bipolar probe with a 5 mm distance tip (60 Hz, pulse width = 0.5 ms, biphasic current, 1–4 s of stimulation) was applied continuously to identify and preserve subcortical sites where interference occurred while the patient performed the HMt using a custom-made intraoperative piece of equipment requiring non-visually guided repetitive object manipulation with the contralesional hand (Fig. 2A). The HMt is effective in mapping functional regions involved in complex hand movement, but also enables quantitative analysis of muscle activity, as the rhythmic movement produces a recurring EMG pattern^{26,33} (Fig. 2B). Interferences in EMG activity of hand and proximal upper limb muscles were concurrently on-line monitored by the neurophysiologist. The current intensity used was the same as was effective in producing HMt interferences during

cortical mapping (mean intensity = 3.3 mA, SD = 0.9 mA) when applied over the premotor cortex. If stimulation disrupted task execution during progression of the resection, the same site was verified by applying DES for two additional non-consecutive times. These sites were reported as ‘effective’. When subcortical stimulation produced a behavioural disturbance, this was reported by the neuropsychologist, and used as landmarks for establishing the functional boundaries of the resection and finally recorded using neuronavigation software (Curve, Brainlab AG, Munich, Germany). Task execution of each patient was videotaped for further offline analysis. To verify the low-frequency DES current threshold, i.e. the minimum intensity required to produce a task interference, each effective site was reassessed with DES by progressively decreasing the current in steps of 0.5 mA.²⁹ Each effective site was also stimulated with high frequency DES and the occurrence of motor evoked potentials in contralateral upper/lower limb and orofacial muscles was evaluated to estimate the distance from the corticospinal tract.³⁵ High frequency DES was delivered using a constant current monopolar stimulator (straight tip, 1.5 mm diameter, Inomed, with reference/ground on the skull overlying the central sulcus)

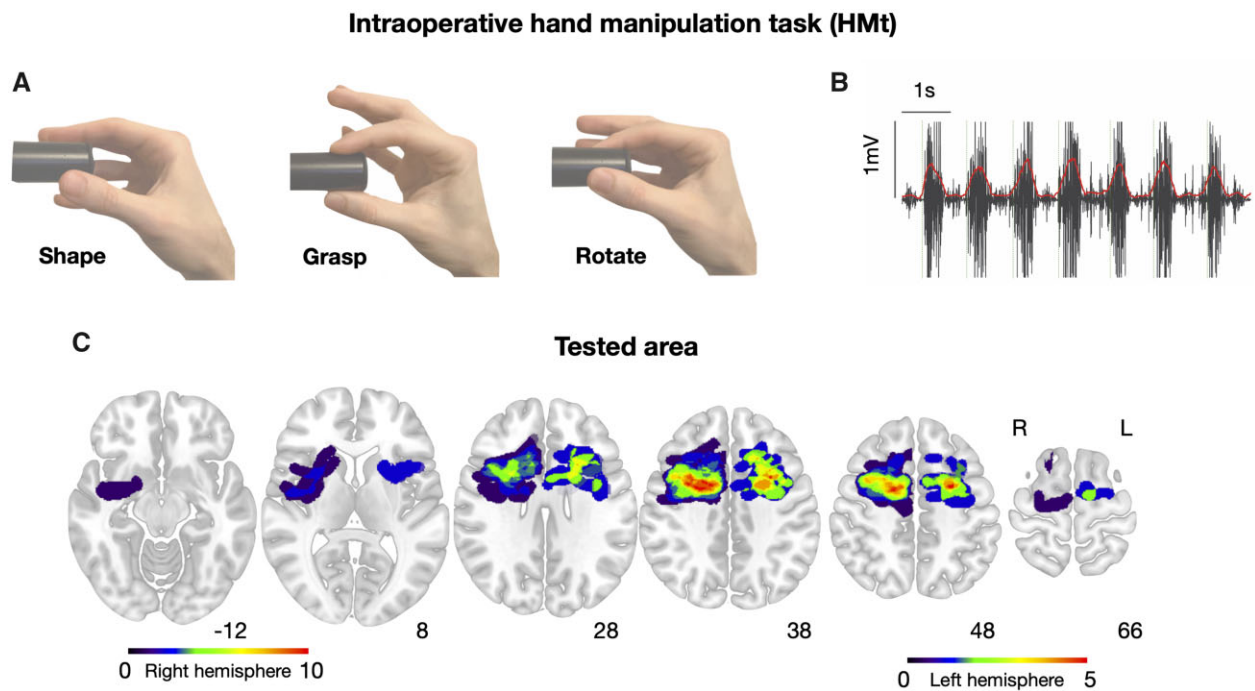


Figure 2 Intraoperative HMT. (A) Representation of the hand manipulation task used in the intraoperative setting, and exemplificative Abductor pollicis brevis EMG pattern (APB; raw signal in black, rectified signal in red) during baseline execution of the task (B). The window between green vertical dashed lines indicates the time used to shape the fingers immediately before the contact with the object, to grasp it, to rotate it and turning back to the initial shaping phase. (C) The common tested area in all patients in the frontal lobe, shown normalized to the MNI template on axial slices.

in trains of five (To5) constant anodal current pulses (pulse duration: 5 ms, interstimulus interval ISI: 3–4 ms). Free-running EMG was recorded through all the procedure. Subdural electrocortigraphy of the precentral gyrus was recorded to detect DES-related afterdischarges or clinical seizures.

Offline EMG analysis

Each subcortical effective site identified during intraoperative HMT was inspected offline using the synchronized EMG recording and the video recording of the behavioural execution. EMG-interference pattern associated to each effective site has been characterized by means of autocorrelation coefficient (aCC) and muscle recruitment analysis (root mean square of EMG signal). Both parameters were calculated for abductor pollicis brevis, extensor digitorum communis and flexor dorsal interosseus, being the main intrinsic and extrinsic muscles involved in task execution.

ACC analysis was used to quantify the effect of DES on the regularity of phasic muscle contractions. The output results of aCC analysis for each muscle ranged from 0 (total loss of rhythmicity) to 1 (sustained rhythmicity). We then classified each effective site based on aCC average value among muscles in two EMG-interference patterns: arrest pattern (aCC = 0), reflecting a behavioural complete arrest of task execution (Supplementary Videos 1 and 2), or clumsy pattern (aCC > 0), referring to a spectrum of disruption of the phasic movement characterized by a progressive slowdown and/or loss of fingers coordination (Supplementary Videos 3 and 4).²⁶

The root mean square of the EMG signal was used to quantify the effect of DES on motor unit recruitment. For each effective site and for each muscle, the root mean square was calculated and then normalized with respect to the root mean square value of the same muscle during baseline movement (in absence of DES). Finally, for each effective site, the root mean square was averaged among muscles. Effective sites were defined as ‘negative’ or

‘positive’ when the root mean square fell below or above the baseline respectively. Only negative effective sites were analysed in this study.

Magnetic resonance data

Data acquisition

All patients underwent MRI 1 day before surgery and at 1-month follow-up. Preoperative MRI was performed on a Philips Intera 3 T scanner (Koninklijke Philips N.V.), and acquired for lesion morphological characterization and volumetric assessment. Fifteen patients underwent a high angular resolution diffusion imaging-optimized diffusion imaging sequence using an eight-channel head coil. A spin echo, single shot echo-planar imaging sequence was performed with 73 directions collected using a b-value of 2000 s/mm^3 , and seven interleaved non-diffusion weighted (b_0) volumes (TE: 96 ms, TR: 10.4 ms). The acquisition had a matrix size of 128×128 with an isotropic voxel size of 2 mm^3 .

Extent of resection

Extent of resection (volume resected with respect to tumour volume) was calculated on postoperative postcontrast MRI for enhancing lesions (target of resection) or FLAIR for nonenhancing lesions (target of resection) and classified on the basis of residual tumour volume as total (residual tumour volume = 0), subtotal (residual tumour volume $\leq 5 \text{ ml}$), and partial (residual tumour volume > 5 ml). A supratotal resection was defined as the complete removal of any signal abnormalities, with the volume of the postoperative cavity larger than preoperative tumour volume.^{31,36}

Registration of intraoperative stimulation sites

The spatial extent of the tested white matter area for each patient was evaluated during the intraoperative procedure on the

preoperative T₁/FLAIR used for neuronavigation and confirmed comparing the posterior border of the resection using the postoperative (1 month) MR image.

All effective sites were recorded by Brainlab software during the intraoperative procedure on the preoperative T₁/FLAIR and confirmed extra-operatively using comparisons between the EMG and video-recordings of the resection and task execution. Resection cavities were delineated on the postoperative (1 month) MR image using ITK-SNAP, and both registered to a common template by means of lesion masking approach using the Clinical Toolbox in SPM (enantiomorphic normalization). Reliability of the normalization process was visually inspected case-by-case. Sites were compared with the border of resection by the operating neurosurgeons (L.B., M.R.). Details of the registration procedure are reported in the [Supplementary material](#).

Probability density estimation of effective sites

The region of highest probability of producing a given EMG-interference pattern was calculated using probability density estimations²⁶ (PDEs; see [Supplementary material](#)).

The PDEs for each hemisphere for arrest and clumsy pattern independently was computed. This map represents a 4D visualization of the anatomical region with the highest probability of inducing a given EMG-interference pattern, based on concentration of stimulation sites. A Dice coefficient of similarity, where 0 indicates no overlap and 1 indicates perfect overlap,^{37,38} was used to compare the overlap between the PDEs for arrest pattern and clumsy pattern within hemispheres, using the PDE thresholded between 15% and 85%.

Disconnectome analysis

To investigate white matter regions corresponding to different EMG-interference patterns, a disconnectome analysis was performed using each effective site as region of interest. Following normalization to MNI space, a 6 mm sphere was centred on the coordinates of each effective site in each patient. The sphere diameter was set in line with the proposed extent of stimulation of the bipolar probe.³⁹ Disconnectome maps were generated from the region of interest spheres for each patient using the Brain connectivity and behaviour (BCB)toolkit.²⁵ If an individual patient experienced the same effect at more than one site, both sites were used to generate the disconnectome map; however, when more than one EMG-interference pattern was identified in different sites in the same patient, separate disconnectome maps were generated for each effect. The maps were generated from the tractography of 20 unrelated right-handed adults processed from the Human connectome project 7-T data release as part of BCBtoolkit ([Supplementary Table 1](#)). This software tracks all white matter streamlines running through the responsive sites of each patient, to produce a percentage overlap map accounting for interindividual variability between the healthy control.²⁵ The disconnectome maps generate voxels showing the probability of disconnection from 0% to 100%. Each patient's disconnection profile was then used to investigate if specific white matter volumes would predict different EMG-interference patterns. To do so, nonparametric statistics were performed on disconnection maps thresholded at 90%, using FSL's randomise tool with 5000 permutations and threshold-free cluster enhancement to correct for multiple comparisons.⁴⁰ One sample t-tests were used with variance smoothing to assess which disconnection profiles were associated with the different EMG-interference pattern, in each hemisphere. The family-wise error threshold was set at $P < 0.05$. To identify the involved white matter tracts, we superimposed the FSL-randomise outputs (contrast maps) with a white matter atlas computed on 1065 healthy

subject⁴¹ (WU-Minn Human connectome project consortium data). For the specific purpose of the study, the Human connectome project corticospinal projections were further dissected using the regions of interest extracted from the Human motor template^{42,43} in the following subcomponents: (i) M1-corticospinal tract (CST); (ii) dorsal premotor cortex corticospinal tract (dPM-CST); (iii) ventral premotor cortex corticospinal tract (vPM-CST); and (iv) supplementary motor area corticospinal tract (SMA-CST). We quantified the involved tracts based on the number of streamlines passing through the contrast maps out of the total amount of streamlines within the specific tracts. Results were expressed as a percentage of disconnected streamlines.

Diffusion tractography in individual patients

As the growth of brain tumours distorts anatomy, we tested and refined the disconnectome results in a subset of 15 patients, comparing their stimulation sites (6 mm-spherical regions of interest) with their preoperative tractogram. Spherical deconvolution modelling and whole brain deterministic tractography was performed using StarTrack software. Virtual dissections of the white matter tracts highlighted by the previous analysis were performed by the first authors (H.H. and L.V.) using a region of interest-based approach, defining regions of interest around regions of white matter reflecting the core of each tract. This included: projection fibres of (i) M1-CST; (ii) dPM-CST; (iii) vPM-CST; and (iv) SMA-CST; striatal fibres of the superior frontal gyrus and the inferior frontal gyrus; association fibres including local u-shaped fibres connecting the middle frontal gyrus to the precentral gyrus (mid-U), the three branches of the superior-longitudinal fasciculus (SLFI, II and III), the frontal aslant tract and the arcuate fasciculus. This allows for visualization of all fibres of a single tract without constraining its cortical projections, which may vary between subjects. Detailed description of the approach to tract dissection is described in previous studies.^{15,24} Both the pre and postoperative T₁ were registered to the spherical deconvolution anisotropic power diffusion map^{44,45} for correct placement of the stimulation site on the tractogram.

Lesion symptom mapping and tract disconnection

In the postoperative phase (5 days from surgery), we assessed the presence of upper-limb motor impairment, using the MRC scale of muscle strength. To associate the postoperative deficits with resected voxels we used a multivariate SVR-LSM using a MATLAB toolbox released by DeMarco and Turkeltaub.⁴⁶ Two dependent variables were separately analysed: (i) the MRC score for motor deficits; and (ii) the De Renzi test score which assess the upper-limb ideomotor apraxia. During the test, patients were asked to imitate a variety (10 items) of intransitive gestures (not requiring the use of objects) with both the arm ipsilateral and that contralateral to the resection. No verbal description of the movements to be imitated was suggested. When an item was not reproduced correctly on the first demonstration, a second demonstration was given. Each item that was performed flawlessly on the first or second demonstration was scored 2 or 1, respectively; in case of unsatisfactory reproduction, the item was scored 0.⁴⁷ Only voxels resected in over 10% of patients were considered. Cluster-level family-wise error correction using permutation testing was applied (5000 permutations; statistical significance $P = 0.05$). As resection volume can be a confounding factor in voxel-behaviour correlations, we controlled for this using a direct total lesion volume control.⁴⁸ The significant cluster was compared with the AAL atlas⁴⁹ and an atlas of white matter.⁴¹ In patients with tractography, the resection cavities were used as exclusion regions of

interest within TrackVis software to calculate the percentage of streamlines remaining for each tract.

Data availability

The data that support the findings of this study are available from the corresponding author, upon reasonable request. The metadata generated in this study are available through Mendeley Data at: doi: 10.17632/xpbct2hw2v.1.

Results

Anatomical and demographic characteristics

Thirty-four patients were included in the study. Patient demographics are summarized in Table 1 (mean age 42 years, SD 10.6; 17 male, four left-handers). In 23 patients a supratotal resection and in 11 a total resection was performed.

Anatomically segregated effects of DES on hand muscles

Although the right frontal white matter was explored more than the left due to functional (language) constraints, a common area

tested in both hemispheres was clearly detected and involved the deep white matter above (3 cm) the central sulcus (Fig. 2C). Within the stimulated area, the arrest pattern (aCC = 0) was found in 36 sites (54%; 27 in right and nine in left hemisphere), while the clumsy pattern (aCC > 0) was found in 30 sites (46%, 15 in right and 15 in left hemisphere) (Fig. 3A–C). In 11 patients, both patterns were observed at different sites. Although muscle suppression occurred in both patterns, when arrest occurred the suppression was significantly higher and affected all muscles (Mann-Whitney U-test, $U = 178$, $P = < 0.0001$). The distribution of aCC and RMS values for each effective site is reported in Supplementary material. Notably, when reducing the current intensity below threshold by 0.5 mA, low frequency DES stimulation of each eloquent site failed in evoking any task interference both at behavioural and EMG level showing that the features of the EMG-patterns were not changing according to the intensity of current used.

When effective sites were stimulated with high frequency DES (To5) up to 10 mA of intensity, no upper-limb motor evoked potentials were never elicited, suggesting a distance of at least 10 mm to the M1-CST.^{35,50–53} An additional analysis showing the distance between the stimulation sites and the trajectory of the M1-CST is reported in Supplementary material.

Anatomical localization of the arrest and clumsy patterns were computed by means of probability density estimation in each

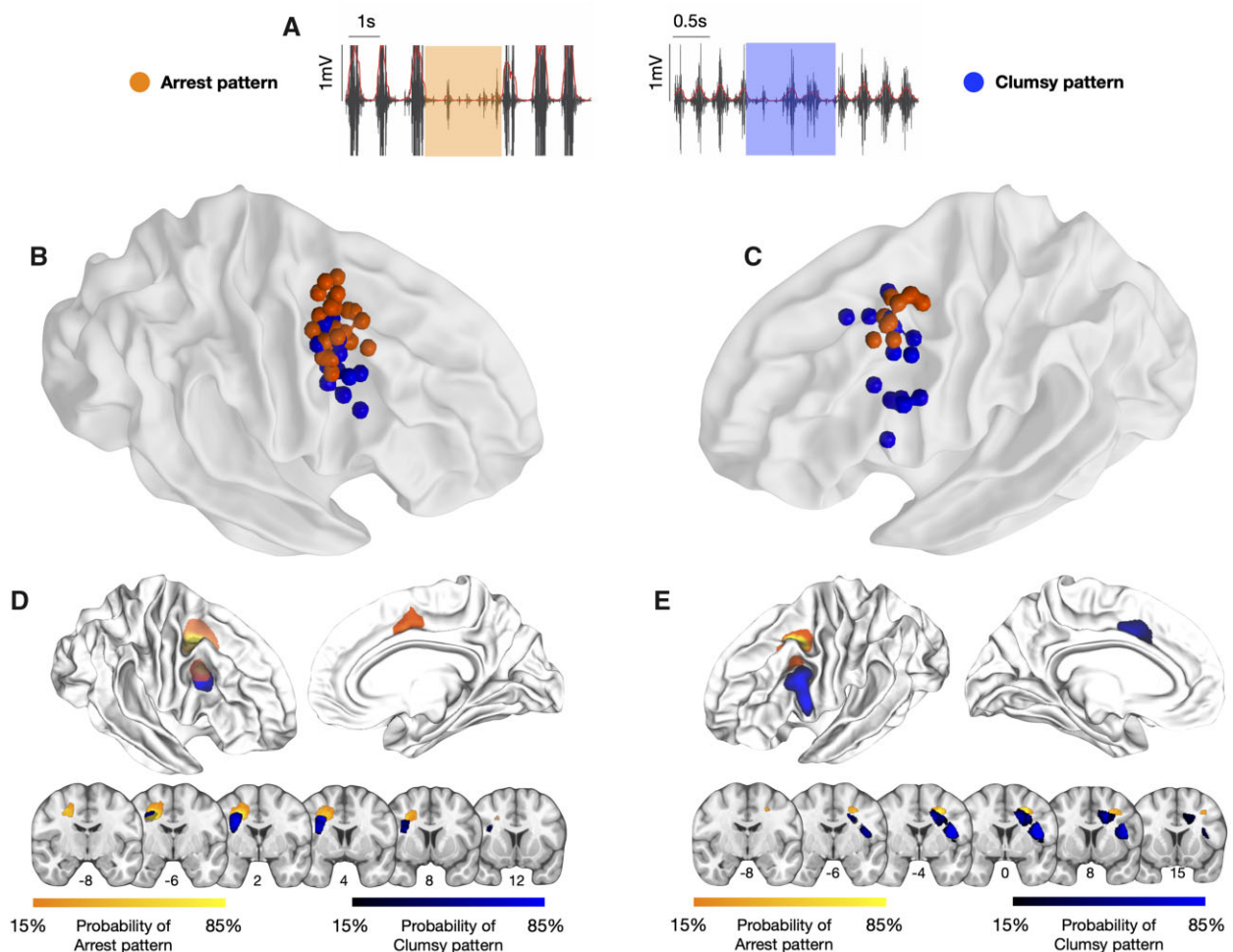


Figure 3 Anatomically segregated effects of DES on object manipulation using EMG pattern analysis. (A) Abductor pollicis brevis activity (APB; raw signal in black, rectified signal in red) during an arrest pattern (left, in orange) and a clumsy pattern (right, in blue). The orange and blue shadows represent the onset and offset of stimulations. (B and C) Distribution of stimulation sites in right and left hemisphere based on aCC value (orange = arrest pattern; blue = clumsy pattern) normalized to the MNI template. (D and E) Probability density estimation of EMG-interference patterns (arrest pattern in orange, clumsy in blue) shown on a right and left 3D white matter MNI reconstruction and on coronal MNI slices.

hemisphere. The two patterns were partially overlapped mainly below the middle frontal gyrus (right hemisphere Dice coefficient = 0.42, left hemisphere Dice coefficient = 0.09). However, the two patterns showed a preferential dorso-ventral distribution: (i) the arrest pattern occurred bilaterally in the white matter below the dorsal premotor region (Fig. 3B–D); and (ii) the clumsy pattern occurred bilaterally in the white matter below the ventral premotor region, and, only in the left hemisphere, four sites out of 15 were reported in the middle anterior cingulum below the pre-SMA (Fig. 3C–E). This distribution was confirmed also in the 11 patients in which both patterns were recorded.

Structural connections linked to different EMG-interference patterns

Disconnectome results

Disconnectome probability maps were created for each patient. Non-parametric one-sample t-tests were run across patients to identify the white matter connections associated with the arrest or the clumsy pattern. Regression showed a dorso-ventral distribution reflecting the results of the probability density estimation (Fig. 3D and E) (see previous section): in both hemispheres, the arrest pattern was associated with the disconnection of dorsal-mesial white matter, while the clumsy pattern with ventral white matter (threshold-free cluster enhancement, $P_{\text{fwer}} < 0.05$) (Fig. 4A and B). After comparison with a white matter atlas,⁴¹ we quantified the percentage of disconnected streamlines for each tract possibly running through this region (Fig. 4C–H and Supplementary Table 2). The tracts most often recruited included association fibres: short U-shaped precentral tracts (mid-U-shaped), the SLF (I, II and III branches), the frontal aslant tract, the arcuate fasciculus; projection fibres: the superior and inferior frontostriatal tracts (FSTs), projections between the cerebral peduncle and (i) the primary motor cortex (M1-CST); (ii) the dorsal premotor cortex (dPM-CST); (iii) the ventral premotor cortex (vPM-CST); and (iv) the supplementary motor area (SMA-CST); and callosal fibres (although these were not further analysed). Short range premotor mid-U-shaped fibres were exclusively associated with the arrest pattern, while inferior fronto-striatal fibres and the superior longitudinal fasciculus III were uniquely associated with the clumsy pattern. Despite the significant structural segregation, a set of common pathways were associated to both effects, including the superior fronto-striatal tract, corticospinal projections, the frontal aslant tract, the arcuate and the superior longitudinal fasciculus I and II.

Individual patients tractography results

The tracts identified with the disconnectome analysis were reconstructed by tractography in a subset of 15 patients (Table 2; seven left hemisphere; eight right hemisphere). In these patients, 27 sites were identified: in 15 sites (four left hemisphere, 11 right) DES induced arrest pattern, in 12 (five left hemisphere, seven right) a clumsy pattern. The location of each site was crossed by dissected tracts in all cases, except for M1-CST and vPM-CST.

Considering white matter variability due to individual differences and possible tract dislocation due to tumour growth, the dissection of tracts at the individual subject level and correlation with stimulation sites improved the reliability and specificity of results. Results clearly showed that stimulation affected tracts running in the frontal white matter below dorsal premotor, producing the arrest pattern, and that stimulation of tracts in the frontal white matter below ventral premotor produced the clumsy pattern. This confirmed the results of disconnectome analysis and reduced the amount of overlap between effects. To improve the sampling, results were grouped irrespective of hemisphere. Figure 5A shows

the frequencies of the two EMG-interference patterns within the studied tracts and Fig. 5B shows the number of stimulations for each tract and pattern. We considered a single tract to be linked to a specific EMG-interference pattern when the latter was evoked by more than 80% of stimulation occurrences with the given tract. Tracts associated with the arrest pattern were the mid-U-shaped fibres, the superior longitudinal fasciculus II (10 of 11 stimulations), the superior fronto-striatal tract (9 of 11 stimulations), the dPM-CST fibres (five stimulations out of six), the SMA-CST fibres (seven of eight stimulations) and the superior longitudinal fasciculus I (six of six stimulations) (Fig. 5C). The clumsy pattern was associated with the superior longitudinal fasciculus III and the arcuate fasciculus (eight of eight stimulations) and with the inferior fronto-striatal tract (seven of seven stimulations) (Fig. 5D). The frontal aslant tract was linked to both arrest pattern (5 of 13 stimulations) and clumsy pattern (8 of 13 stimulations) (Fig. 5E). No effective site was located within the trajectory of the M1-CST and vPM-CST. Figure 5F–J shows a patient with multiple stimulation sites and their relationship with white matter tracts.

Resection of dorsal white matter was associated to transient postoperative upper-limb motor deficit

Eleven patients out of 34 experienced transient postoperative MRC deficits at 5 days from surgery, completely recovered at the 1-month follow up (Table 1). Figure 6A reports the common resected area in all patients. SVR-LSM showed the association of the MRC deficit with a cluster of voxels located in the white matter below the right superior frontal gyrus, including the SMA, mesial to the mid-anterior cingulate cortex (mACC) ($P = 0.05$; 5000 permutations, Fig. 6B). In the left hemisphere only three patients experienced postoperative MRC deficits, thus no significant voxels emerged. The significant cluster overlapped only with the arrest pattern density map (134 voxels in common) and corresponded with the dorsal white matter region enclosing mainly SMA-projections and the superior fronto-striatal tracts (Fig. 6C and D). No overlap emerged with the region where DES elicited the clumsy pattern. Finally, we evaluated the impact of resection on the 11 investigated tracts in the 15 patients with tractography. In this group, only three patients experienced transient MRC deficits. In all of this group over 50% of resection cavities enclosed the dorsal frontal white matter region, including mid-U-shaped fibres, SMA-CST and superior fronto-striatal fibres. Notably, in all 15 patients, the frontal aslant tract, the three branches of the superior longitudinal fasciculus, the arcuate and the inferior fronto-striatal tract were commonly resected without any association with MRC upper-limb deficit or apraxia (Fig. 6E). M1-CST and vPM-CST were never resected in any patient. In addition to MRC evaluation, we also performed a SVR-LSM for upper-limb ideomotor apraxia. We excluded the patients with postoperative MRC deficits from this analysis. In both hemispheres no significant clusters emerged. Only one patient had a pathological score in the De Renzi test in the immediate postoperative phase (Table 1), which fully recovered at the 1-month follow-up. This observation is consistent with previous findings showing that surgery guided by intraoperative HMT reduces immediate and long-term postoperative praxis deficits.³³

Discussion

In this study we aimed at identifying the frontal lobe connections involved in hand-muscle control during the performance of an ecologically relevant hand-object manipulation task, by using subcortical DES during the awake phase of neurosurgical procedures of 34 patients. Results of the intraoperative brain mapping, EMG-interference pattern analysis and diffusion tractography point to

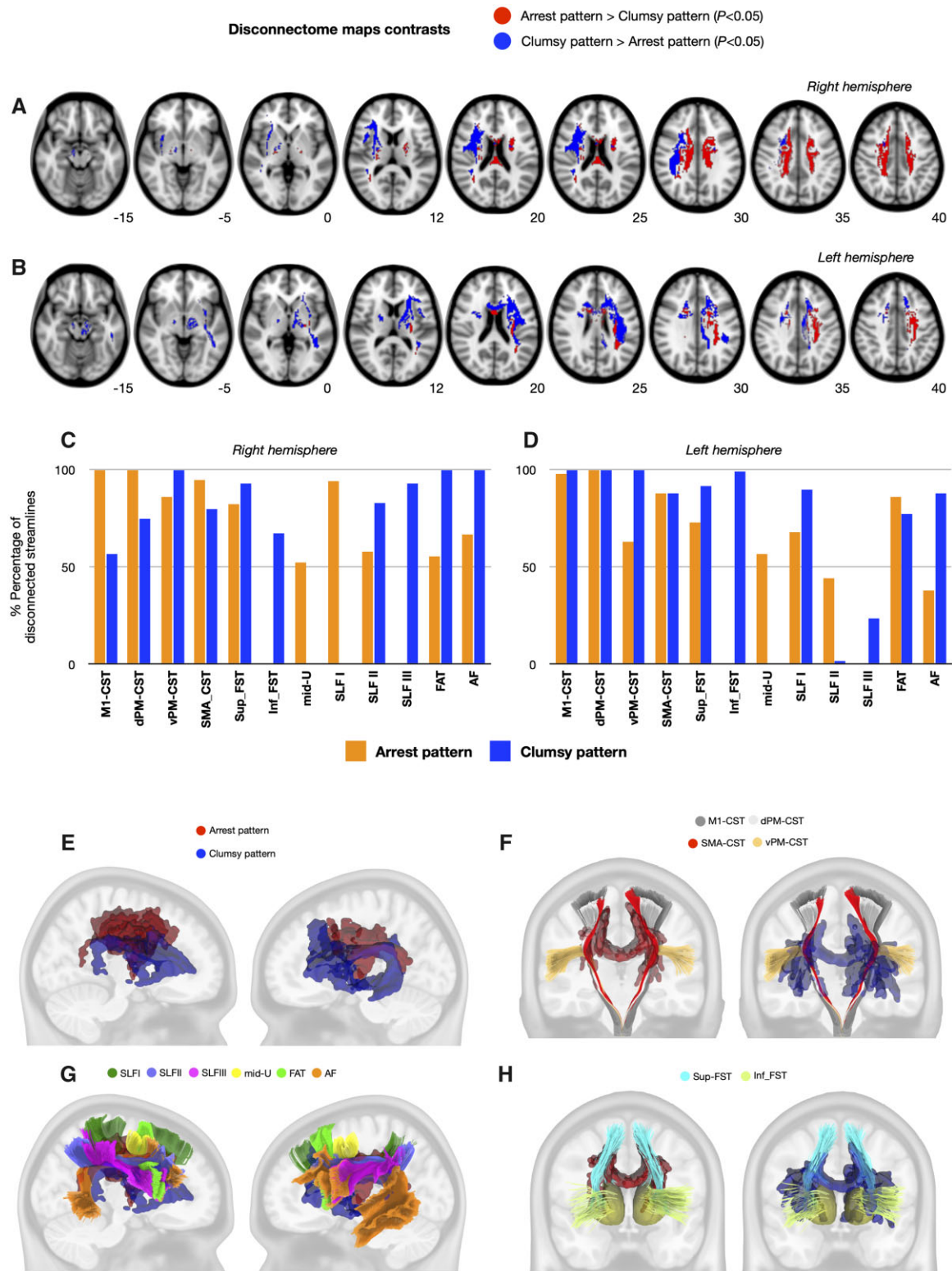


Figure 4 Disconnectome maps associated with EMG-interference patterns. Statistical disconnectome maps (threshold-free cluster enhancement, P -value < 0.05) predicting the arrest pattern (red) or the clumsy pattern (blue) shown on normalized axial slices in the right (A) and left (B) hemisphere. Percentage of overlap between the statistical disconnectome maps and white matter tracts from a healthy population atlas (Yeh *et al.*⁴¹) in the right (C) and left (D) hemisphere (callosal fibres not shown). 3D renderings of the right and left disconnectome maps (E). On axial slices is shown the overlap between the disconnectome maps and both corticospinal (F) and striatal fibres (H). The sagittal slices show the overlap between the disconnectome maps and the association tracts (G).

Table 2 Diffusion tractography of 15 patients

No	Hem	M1-CST	dPM-CST	vPM-CST	SMA-CST	Sup-FST	Inf-FST	mid-U	SLFI	SLFII	SLFIII	FAT	AF
20	R	5.5	3.4a	1.6	8.5a	11.4a	0.56	1.52a	22.1a	8.691a	17.1	7.4a	3.23
21	L	8.3	5.5	5.1	10.3a	10.1a	1.6	2.46a	17.1	22.6a	15.4	19.1a	8.9
22	L	11.7	4.2a	2.9	7.7a	2.8a	3.3c	6.1a	9.0a	9.34	11.1c	4.2a, c	9.6c
23	R	4	3.9a	2.8	7.6a, c	4.39a, c	3.03c	9.2a, c	18.9	21.8a, c	20.3c	1.6c	7.9c
24	R	8.6	4.3a	0.4	9.1	8.3a, c	11.1	2.6a	19.8	10.2a	21.7c	11.5c	10.9c
25	R	6.1	2	2.7	10.1a	4.9a	11.4	13.2a	26.3a	16.3a	25.4	9.2	5.6
26	L	6	5.4	0.4	10.6	4.7	0.4	6.1a	13.1a	13.6a	24.5	6.7	15.2
27	R	4.3	4.5	0.4	12.3a	6.2a	3.2c	5.2	25.6a	27.6a	19.5c	8.35a, c	9.4c
28	R	5.4	4.4	2.3	6.6	2.8	5.4	4.1a	28.2	21.1a	27.3	11.9	10.9
29	L	7.5	5.9	0.8	7	2.9	3.1c	2.4	21.9	19.9	8.6c	9.8c	3.9c
30	R	4.7	3.7	9.1	8.9	0.5	10.1c	2.4	22.5	17.5	19.3c	8.3	9.9c
31	L	5.8	4	2.4	5.7a	2.4a	1.6	6.3a	12.8a	9.7a	15.4	17.8a	8.9
32	L	8.2	4.2	2.9	10.7	3.9	1.8c	4.2	18.5	19.2	12.4c	12.3c	18.5c
33	L	3.7	1.4	3.9	4.9	1.9	12.3c	8.3	22.2	10.8	26.1c	9.5c	24.6c
34	R	15.6	8.4a, c	4	7.5	0.8a	5.2	3.13a	32.03	19.2a	16.7	12.3c	5.11

Measurements are expressed in millilitres. a = arrest pattern; c = clumsy pattern. Sup_FST = superior FST; Inf_FST = inferior FST; FAT = frontal aslant tract; AF = arcuate fasciculus.

the existence of two different white matter regions associated to distinct aspect of task-related motor output implementation. We evaluated the effect of permanent disconnection of different white matter tracts on immediate postoperative motor outcome using two commonly used clinical tests, the MRC scale of muscle strength and the De Renzi test for ideomotor apraxia. The preservation during surgery of dorsal white matter surrounding the supplementary motor area is crucial to preserve upper-limb movement integrity in the immediate postoperative phase, although in the ventral region no motor deficit was detected with these clinical tests.

Probability density estimation of EMG-interference patterns

DES evoked either complete disruption of hand-muscle activity required for task execution (arrest pattern), or a partial disruption consisting of a spectrum of milder effects ranging from movement slowdown to a loss of finger coordination (clumsy pattern). Localization based on probability density estimation (PDE) of the two interference patterns showed that, although they overlapped below the middle frontal gyrus, the arrest pattern occurred preferentially during stimulation of white matter below a dorsal premotor region anterior to the precentral hand-knob, whereas the clumsy pattern occurred preferentially within white matter below ventral premotor region. In a previous study adopting the same methodological approach to investigate cortical premotor areas similar EMG-interference patterns were identified on the precentral convexity.²⁴ The arrest pattern was reported in both vPM and dPM, although in the latter it was associated with mixed suppression-recruitment effects (an initial period of muscle suppression followed by a progressive recruitment of motor units). The clumsy pattern was instead reported exclusively in vPM, with different degrees of muscle suppression. The homologies and differences emerging along the dorso-ventral direction with the present study might be due to differences in the neural elements stimulated with DES (cortical versus subcortical). Stimulation can evoke inhibitory or excitatory effects within local neuronal populations depending on its proximity to grey or white matter.⁵⁴ Despite local and remote neurophysiological effects induced by DES are still poorly understood, in line with the previous study,²⁶ we suggest that the two EMG-interference patterns may result from stimulation of different neuronal substrates: the arrest pattern may reflect

the disruption of a network closely involved in motor output implementation, while the clumsy pattern may reflect the perturbation of a network possibly involved in sensorimotor computations required for task execution.

Disconnectome and tractography in single patients

To predict which white matter connections were associated to the different EMG-interference patterns, we used a disconnectome analysis,²⁵ assuming that DES caused a transient disconnection of the workflow information between interconnected structures. The arrest and clumsy patterns were associated respectively with disconnection of different dorsal and ventral white matter pathways, in line with the results shown by PDE. Within these regions, we identified specific and common white matter tracts for the two interference patterns. Short range premotor mid-U-shaped fibres were only associated with the arrest pattern, while inferior fronto-striatal fibres and the superior longitudinal fasciculus III were uniquely associated with the clumsy pattern. Despite the significant structural segregation, both effects could result from the interference of the activity of corticospinal fibres from primary and premotor areas. Permanent disconnection of these fibres has been extensively correlated to deficits in dexterity.^{55–57} Moreover, a set of common striatal and associative pathways, including the superior fronto-striatal tract, the frontal aslant tract, the arcuate and the superior longitudinal fasciculus I and II, were correlated to both effects.

To improve the specificity of the atlas-based disconnectome results, we used preoperative tractography in 15 patients to assess the disconnected tracts based on their own stimulation sites. This analysis refined the previous results to show that: (i) transient disconnection of dorsal white matter including local mid-U-shaped fibres together with the superior longitudinal fasciculus I and II, the superior fronto-striatal tract and corticospinal projections of dPM and SMA was preferentially associated with the arrest pattern; (ii) transient disconnection of ventral white matter, including the inferior fronto-striatal tract, the superior longitudinal fasciculus III and the arcuate instead produced the clumsy pattern; and (iii) precentral corticospinal fibres (linked to M1 and vPM) were not affected by stimulation, as no sites were in the vicinity of these connections. The dorsal region, differently from the ventral one, has direct access to the spinal cord via SMA/dorsal PM-CST and both direct/indirect connections with primary motor output via

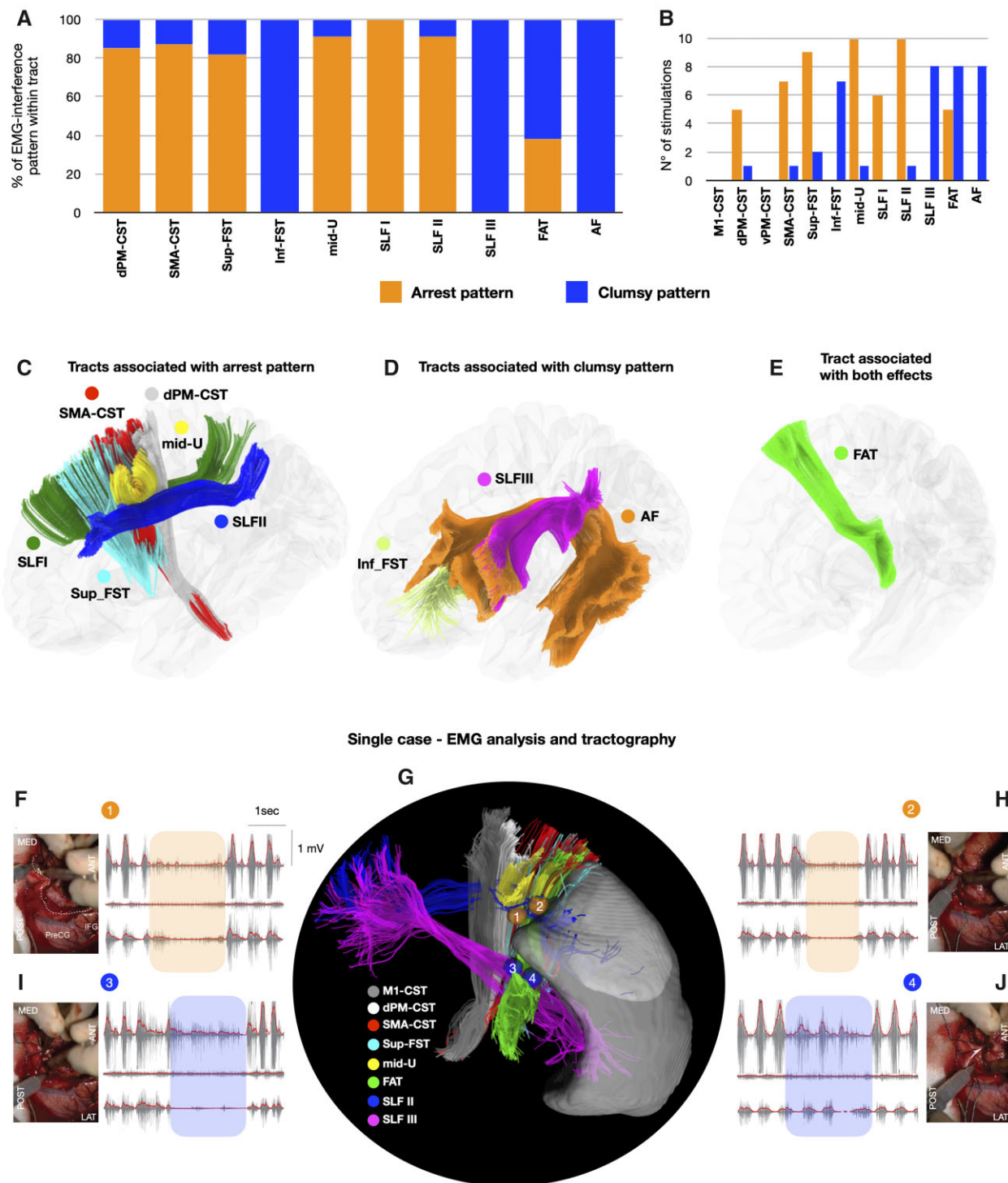


Figure 5 White matter tracts associated with different stimulation effects—single subject diffusion tractography. (A) Bar graph shows the percentage of stimulations, within tract, producing the arrest or the clumsy pattern. (B) Bar graph shows the total number of stimulations for each tract. All tracts are represented on normalized templates, divided based on their likelihood to be associated with arrest pattern (C) or clumsy pattern (D). The frontal aslant tract was associated to both effects (E). The lower panel shows a single patient who underwent surgery for a right frontal anaplastic oligodendroglioma (grade III) who did not experience a postoperative deficit. Screenshot from surgical video taken during subcortical stimulation and corresponding EMG interference patterns are reported for multiple sites. Arrest pattern was elicited in site 1 (F, aCC = 0, root mean squared (RMS) = 45% compared to baseline) and in site 2 (H, aCC = 0, RMS = 31% compared to baseline). Clumsy pattern was elicited in site 3 (I, aCC = 0.3, RMS = 45% compared to baseline) and in site 4 (J, aCC = 0.9, RMS = 69% compared to baseline). These sites are shown relative to the underlying white matter anatomy of the patient (G), traced using diffusion tractography. Resection cavity (dark grey) and tumour (light grey) are overlaid in the same space.

basal ganglia-thalamo-cortical loops and local motor-premotor U-shaped fibres. This result agrees with the hypothesis that the arrest pattern may reflect the perturbation of a network

hierarchically proximal to the motor output. Coherently, lesion analysis showed that resection of the dorsal white matter region (i.e. mid-U fibres, SMA projections and superior-FST), but not of

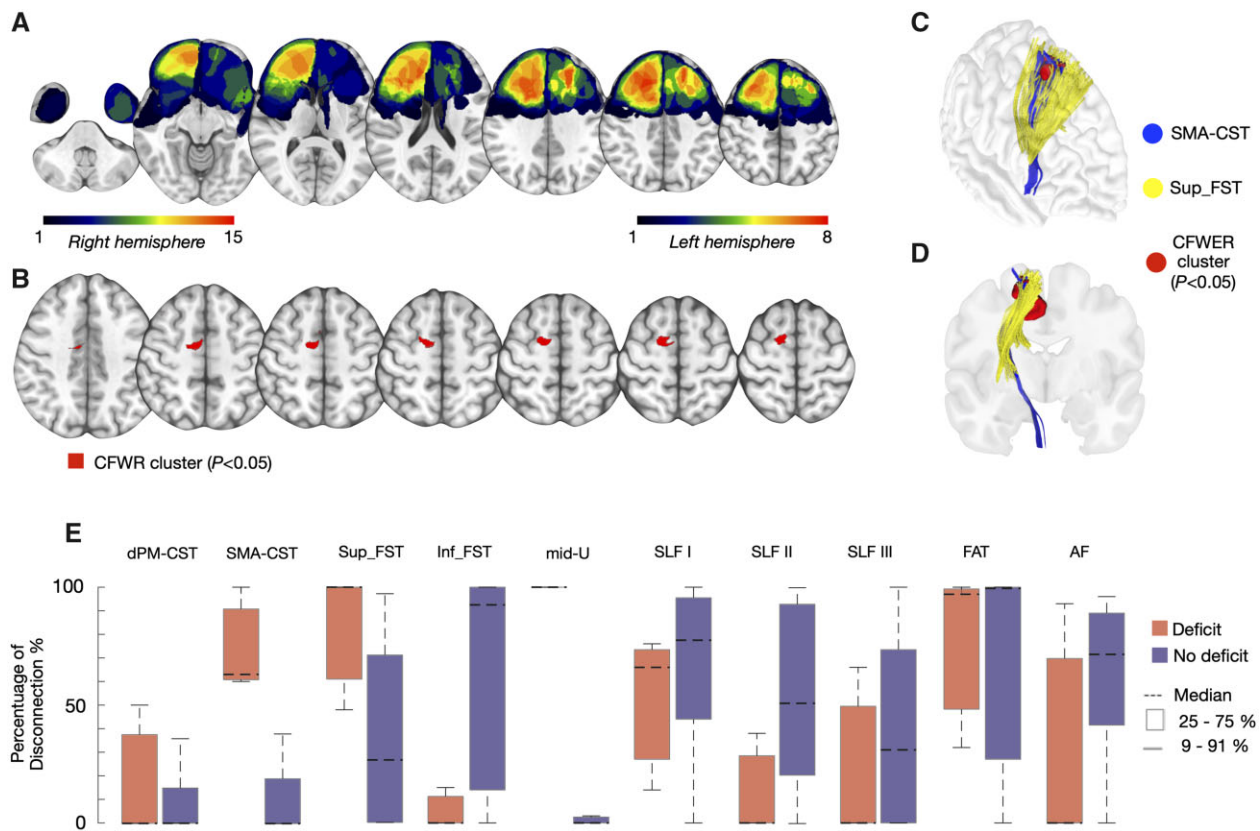


Figure 6 Effect of resection on immediate postoperative motor outcome. (A) Overlap maps of resection cavities of all patients. (B) Significant cluster associated with a decrease in upper-limb motor performance (5 days post-surgery, MRC score). This cluster is also displayed in 3D reconstructions showing its overlapping with the projection fibres from the SMA and the superior FST (C and D). (E) Percentage of streamlines disconnected by the neurosurgical procedure for each tract in the 15 patients with tractography. Motor outcome is compared between the three patients with transient MRC deficit (red) and those without deficits (blue).

the ventral one, was significantly associated with short-term MRC postoperative upper limb deficit.

Arrest of movement occurs stimulating white matter below dorsal premotor area

The arrest pattern occurred when DES was applied below dorsal premotor cortex where cortico-fugal, cortico-striatal, and cortico-cortical projections intersect. Although this study does not provide conclusive evidence whether the effect induced by DES results from the stimulation of one or multiple white matter pathways, non-human primate studies may suggest some interpretations.

Since no muscle contractions were elicited when stimulating the hand at rest within this region, nor even when stimulating with high frequency DES and progressively increasing current intensity (until 10 mA, an intensity corresponding approximately to a distance of 10 mm to the CST^{35,50–53}) we reasonably ruled out the involvement of the corticospinal tract originating from the primary motor area. However, as also highlighted by tractography results, projections descending from the dPM and the SMA should be considered. In non-human primates, the SMA and dPM have direct access to the spinal cord, with dense terminations to inhibitory interneurons of the intermediate zone, mainly in lateral lamina VII.^{58,59} Coherently, DES applied in a region dense with cortico-fugal fibres may have caused abnormal activation of inhibitory spinal circuits leading to the muscle suppression observed in the task arrest pattern. In accordance with this hypothesis, optogenetic stimulation of spinal inhibitory interneurons arrests the voluntary motor output.⁶⁰

Inhibition of ongoing upper limb movement occurs in non-human primates during stimulation of white matter superior to the dorsal striatum.^{61,62} Direct and indirect cortico-thalamic loops via the basal ganglia guarantee motor inhibition, a key component of adaptive behaviour.^{3,63,64} In our cohort of patients, stimulation of superior fronto-striatal fibres may have altered the excitatory-inhibitory balance within the basal ganglia circuits, eventually affecting the excitability of the primary motor output. In humans, this hypothesis is coherent with previous intraoperative studies suggesting that the arrest of repetitive flexion-extension of the arm might be induced by stimulation of cortico-striatal tracts.^{65,66}

Short association U-shaped fibres connecting the hand-knob sector of primary motor cortex with the middle frontal gyrus may also have been implicated in facilitating hand-object interaction. In a previous study, using the same task,²⁸ DES of the anterior hand-knob region hosting caudal U-shaped terminations evoked task arrest concomitant to suppression of hand muscles. This preliminary result suggests that these fibres may play an inhibitory role on the primary motor output, an hypothesis supported by non-human primate data reporting a short-latency powerful inhibition of M1 output due to a conditioning stimulation of dPM.⁶⁷ Premotor short association tracts have been identified in humans using postmortem methods,⁶⁸ diffusion tractography^{69,70} and 7 T MRI⁷¹ and have been theorized to be the human homologues of the cortico-cortical premotor connections engaged in the monkey reaching and grasping system.^{69,72}

The dorsal white matter area is also a region crossed by frontoparietal connections recognized to be responsible for different processes of sensorimotor integrations required by hand action in

non-human primates.¹¹ The dorsal branch of the SLF (I) has been linked to manual specialization and lateralized hand selection,^{24,73} while the middle branch (SLFII) seems to be involved in higher order sensorimotor transformation for reaching and grasping and oculomotor exploration.^{23,24,74,75} Possibly, the SLFI/II, in addition to its visuomotor functions, may also transmit relevant proprioceptive and tactile information required for controlling finger coordination during haptically guided object manipulation. However, considering the functional aspects associated with these pathways and that the HMT is performed in absence of visual guidance, it seems not reasonable to hypothesize that DES of the SLFI/II could evoke a massive distal muscle suppression.

Finally, DES may have also perturbed the excitability of the contralateral motor areas via transcallosal fibres connecting the contralateral motor-premotor areas. In this regard, it has been shown that interhemispheric inhibition is a key component in fine dextrous motor control, mediated via motor transcallosal fibres.^{76–78}

Clumsy movement occurs when stimulating white matter below ventral premotor area

The clumsy pattern was characterized by a low level of regularity between phasic muscle contractions and behaviourally shows a progressive movement slowdown and loss of finger coordination. It occurred with highest probability in a white matter region below the ventral premotor area, mainly occupied by fronto-parietal and inferior fronto-striatal connections.

This region contains fibres of the superior longitudinal fasciculus III, connecting the supramarginal gyrus (anterior inferior parietal lobule) with inferior frontal regions.⁷⁹ The disconnectome analysis indicated this fascicle may be affected by stimulation in the right hemisphere only. However, this result may have been influenced by the strong right-ward asymmetry of this tract described in literature.^{23,24,80} In fact, when examining the patients with tractography, we showed that in fact stimulation had affected the SLFIII in both hemispheres. Anatomic-functional studies in non-human primates report this connection as the most likely homologue of the AIP/PFG-F5 circuit underlying grasp-related sensorimotor transformations in macaques.⁵ In the non-human primate, the PFG/AIP connections with the anterior premotor area F5 represent the core of a large-scale network for purposeful hand action, integrating sensorimotor and cognitive information.⁷⁴ Interestingly, using behavioural inspection, the clumsy pattern resembled symptoms associated with myelo/limb-kinetic apraxia.⁸¹ Patients with this disorder cannot accurately realize fine motor acts, such as turning a key into a lock. Limb-kinetic apraxia occurs in frontal lesions and its nature is controversial, as it is difficult to disentangle this higher order deficit from a concurrent limb weakness.⁸² Fogassi and colleagues⁸³ also highlighted the similarity between this condition and impairment in hand-shaping after reversible inactivation of monkey vPM during visually guided grasping in macaques. A similar pattern of interference has been reported in humans when vPM is virtually lesioned by transcranial magnetic stimulation during a precision grip task, which affects accurate finger adjustments on the object.⁸⁴ Notably, the superior longitudinal fasciculus III has cortical terminations in the dorsal sector of vPM, where DES during the HMT evoked the same clumsy pattern.²⁶ Moreover, information coming from the human right and left inferior parietal lobe seem crucial in perception of our own limbs and in somatic perception of hand-object interactive movement respectively.^{85,86} Overall, the effects evoked by DES-related transient disconnection of the superior longitudinal fasciculus III during HMT might reflect disruption of information carried between the parietal and premotor cortex.

Disconnectome and tractography results also showed that the clumsy pattern may have been induced by stimulation of inferior fronto-striatal fibres. Again, these data are coherent with the anatomic-functional organization of the macaque lateral grasping network, where vPM sends inputs to specific sectors of the putamen.⁸⁷ Notably the limb-kinetic apraxia is a symptom of neurodegenerative disorders involving the basal ganglia, such as progressive supranuclear palsy and Parkinson disease. In this view, the apraxic symptoms, and the clumsy pattern observed in the present study, may reflect combined cortico-cortical connections to ventral premotor area and cortico-striatal dysfunction.⁸²

The frontal aslant tract

Finally, the association of the frontal aslant tract with both the arrest and clumsy pattern deserves discussion. The frontal aslant tract is an intra-lobar tract connecting the SMA/preSMA region with the posterior inferior frontal gyrus,⁶⁹ which intersects both the dorsal and ventral regions emerging in our analysis. The double effect associated with the frontal aslant tract may be due to its stimulation at the intersection with the tracts actually mediating the effect, challenging its direct involvement. Alternatively, we speculate that DES delivered along the frontal aslant tract may affect task execution by acting indirectly on the ventral and dorsal node, possibly via their common cortical sources. The functional role of the frontal aslant tract is diverse, being associated with speech and language,⁸⁸ working memory⁸⁹ and visually guided upper-limb movements.⁹⁰ However, the lesion analysis here showed this pathway could be resected without postoperative motor deficit, which may suggest it plays an indirect role in motor output control.

Association between permanent disconnection and motor outcome

Results showed that partial resection of the SMA and surrounding white matter was associated with an immediate postoperative upper-limb motor impairment, fully recovered at the 1-month follow-up. This result is coherent with the transient akinesia or 'SMA syndrome' described in the neurosurgical literature after SMA resection⁹¹ and with human studies predicting motor outcome after stroke based on dorsal premotor white matter integrity.^{92,93} This result was confirmed in a subset of patients with preoperative diffusion tractography. In this cohort, the absence of motor deficit occurred only when SMA-projections and mid-U-shaped connections to M1 were spared. This supports our hypothesis, suggesting a functional proximity of the dorsal white matter region to the hand-related motor output. Overall, our results highlighted the clinical importance of preserving SMA fibres, whose correlation with motor deficit was demonstrated in patients with subcortical stroke.⁵⁵ On the other hand, the frontal aslant tract, the arcuate, the three branches of the superior longitudinal fasciculus and the inferior fronto-striatal fibres were commonly resected without any motor disturbances. Resection of the latter tracts might rather be associated to higher sensorimotor disorders, such as ideomotor apraxia. However, SVR-LSM for this clinical variable did not show, in the sample of patients analysed, any significant clusters, leaving this issue unsolved.

Limitations

The intraoperative setting, while providing a unique opportunity for studying the role of tracts, has some intrinsic limitations. The area to be stimulated in single patients cannot be established *a priori* for research purposes, but entirely depends on the surgical

strategy. For this reason, the left hemisphere was less investigated in terms of the number of stimulation sites, as language tests were also performed to assess the posterior border of the resection. It is also not possible to study subtle hemispheric differences using DES, as patients cannot be tested in both hemispheres. As tumour location and surgical strategy establish the area available for testing with stimulation, it would be important to confirm these results in an even higher number of patients with diffusion tractography and taking advantage of advanced electrophysiological recording techniques.⁹⁴ Finally, our intraoperative task was haptically performed, in order to focus mainly on the motor domain of hand-object manipulation, thus results cannot be attributed to mechanisms underlying visual guidance and/or reaching phase of the movement.

Acknowledgements

We are very grateful to Roger Lemon and Stephanie Forkel for their helpful comments on the manuscript. Data were provided in part from the HCP, WU-Minn Consortium (Principal Investigators: David Van Essen and Kamil Ugurbil; 1U54MH091657) funded by the 16 NIH Institutes and Centers that support the NIH Blueprint for Neuroscience Research; and by the McDonnell Center for Systems Neuroscience at Washington University in St. Louis.

Funding

This work has been supported by ‘Regione Lombardia’ under the Eloquentstim Project (PorFesr, 2014–2020) to G.C. and by a grant from Associazione Italiana per la Ricerca sul Cancro (AIRC) to L.B.

Competing interests

The authors have no conflicting interests to report.

Supplementary material

Supplementary material is available at *Brain* online.

References

1. Almécija S, Smaers JB, Jungers WL. The evolution of human and ape hand proportions. *Nat Commun*. 2015;6(1):1–11.
2. Lemon RN. Descending pathways in motor control. *Annu Rev Neurosci*. 2008;31:195–218.
3. Alexander GE, Crutcher MD. Functional architecture of basal ganglia circuits: Neural substrates of parallel processing. *Trends Neurosci*. 1990;13(7):266–271.
4. Aron AR, Durston S, Eagle DM, Logan GD, Stinear CM, Stuphorn V. Converging evidence for a fronto-basal-ganglia network for inhibitory control of action and cognition. *J Neurosci*. 2007;27(44):11860–11864.
5. Borra E, Gerbella M, Rozzi S, Luppino G. The macaque lateral grasping network: A neural substrate for generating purposeful hand actions. *Neurosci Biobehav Rev*. 2017;75:65–90.
6. Cisek P, Kalaska JF. Neural mechanisms for interacting with a world full of action choices. *Annu Rev Neurosci*. 2010;33:269–298.
7. Ebbsen CL, Brecht M. Motor cortex - To act or not to act? *Nat Rev Neurosci*. 2017;18(11):694–705.
8. Gallivan JP, Chapman CS, Wolpert DM, Flanagan JR. Decision-making in sensorimotor control. *Nat Rev Neurosci*. 2018;19(9):519–534.
9. Thiebaut de Schotten M, Foulon C, Nachev P. Brain disconnections link structural connectivity with function and behaviour. *Nat Commun*. 2020;11(1):1–8.
10. Gharbawie OA, Stepniewska I, Qi H, Kaas JH. Multiple parietal-frontal pathways mediate grasping in macaque monkeys. *J Neurosci*. 2011;31(32):11660–11677.
11. Battaglia-Mayer A, Caminiti R. Corticocortical systems underlying high-order motor control. *J Neurosci*. 2019;39(23):4404–4421.
12. Howells H, Simone L, Borra E, Forna L, Cerri G, Luppino G. Reproducing macaque lateral grasping and oculomotor networks using resting state functional connectivity and diffusion tractography. *Brain Struct Funct*. 2020;225(8):2533–2551.
13. Graziano MSA, Aflalo TN. Mapping behavioral repertoire onto the cortex. *Neuron*. 2007;56(2):239–251.
14. Forna L, Puglisi G, Leonetti A, et al. Direct electrical stimulation of the premotor cortex shuts down awareness of voluntary actions. *Nat Commun*. 2020;11(1):1–11.
15. Catani M, Thiebaut de Schotten M. *Atlas of human brain connections*. Oxford University Press; 2012. doi: 10.1093/med/9780199541164.001.0001
16. Barrett RLC, Dawson M, Dyrby TB, et al. Differences in frontal network anatomy across primate species. *J Neurosci*. 2020;40(10):2094–2107.
17. Coscia M, Wessel MJ, Chaudary U, et al. Neurotechnology-aided interventions for upper limb motor rehabilitation in severe chronic stroke. *Brain*. 2019;142(8):2182–2197.
18. Micera S, Caleo M, Chisari C, Hummel FC, Pedrocchi A. Review advanced neurotechnologies for the restoration of motor function. *Neuron*. 2020;105(4):604–620.
19. Bello L, Riva M, Fava E, et al. Tailoring neurophysiological strategies with clinical context enhances resection and safety and expands indications in gliomas involving motor pathways. *Neuro Oncol*. 2014;16(8):1110–1128.
20. Duffau H. Stimulation mapping of white matter tracts to study brain functional connectivity. *Nat Rev Neurol*. 2015;11(5):255–265.
21. Puglisi G, Howells H, Leonetti A, et al. Frontal pathways in cognitive control: Direct evidence from intraoperative stimulation and diffusion tractography. *Brain*. 2019;142(8):2451–2465.
22. Mori S, Tournier JD. Moving beyond DTI: High Angular Resolution Diffusion Imaging (HARDI). In: Mori S, Tournier JD, eds. *Introduction to diffusion tensor imaging*. Elsevier; 2014:65–78.
23. Budisavljevic S, Dell’Acqua F, Zanatto D, et al. Asymmetry and structure of the fronto-parietal networks underlie visuomotor processing in humans. *Cereb Cortex*. 2017;27(2):1532–1544.
24. Howells H, De Schotten MT, Dell’Acqua F, et al. Frontoparietal tracts linked to lateralized hand preference and manual specialization. *Cereb Cortex*. 2018;28(7):2482–2494.
25. Foulon C, Cerliani L, Kinkingnéhun S, et al. Advanced lesion symptom mapping analyses and implementation as BCBtoolkit. *Gigascience*. 2018;7(3):1–17.
26. Forna L, Rossi M, Rabuffetti M, et al. Direct electrical stimulation of premotor areas: Different effects on hand muscle activity during object manipulation. *Cereb Cortex*. 2020;30(1):391–405.
27. Simone L, Forna L, Viganò L, et al. Large scale networks for human hand-object interaction: Functionally distinct roles for two premotor regions identified intraoperatively. *Neuroimage*. 2020;204:116215.
28. Viganò L, Forna L, Rossi M, et al. Anatomic-functional characterisation of the human “hand-knob”: A direct electrophysiological study. *Cortex*. 2019;113:239–254.
29. Viganò L, Howells H, Forna L, et al. Negative motor responses to direct electrical stimulation: Behavioral assessment hides different effects on muscles. *Cortex*. 2021;137:194–204.

30. Leonetti A, Puglisi G, Rossi M, et al. Factors influencing mood disorders and health related quality of life in adults with glioma: A longitudinal study. *Front Oncol*. 2021;11(1):662039.
31. Rossi M, Gay L, Ambrogi F, et al. Association of supratotal resection with progression-free survival, malignant transformation, and overall survival in lower-grade gliomas. *Neuro Oncol*. 2021; 23(5):812–826.
32. Rossi M, Nibaldi MC, Viganò L, et al. Resection of tumors within the primary motor cortex using high-frequency stimulation: Oncological and functional efficiency of this versatile approach based on clinical conditions. *J Neurosurg*. 2020;133(3):642–654.
33. Rossi M, Fornia L, Puglisi G, et al. Assessment of the praxis circuit in glioma surgery to reduce the incidence of postoperative and long-term apraxia: A new intraoperative test. *J Neurosurg*. 2018;130(1):17–27.
34. Conti Nibaldi M, Leonetti A, Puglisi G, et al. Preserving visual functions during gliomas resection: Feasibility and efficacy of a novel intraoperative task for awake brain surgery. *Front Oncol*. 2020;10:1485.
35. Raabe A, Beck J, Schucht P, Seidel K. Continuous dynamic mapping of the corticospinal tract during surgery of motor eloquent brain tumors: Evaluation of a new method. *J Neurosurg*. 2014; 120(5):1015–1024.
36. Rossi M, Ambrogi F, Gay L, et al. Is supratotal resection achievable in low-grade gliomas? Feasibility, putative factors, safety, and functional outcome. *J Neurosurg*. 2019;132(6):1692–1705.
37. Dice LR. Measures of the amount of ecologic association between species. *Ecology*. 1945;26(3):297–302.
38. Zou KH, Warfield SK, Bharatha A, et al. Statistical validation of image segmentation quality based on a spatial overlap index. *Acad Radiol*. 2004;11(2):178–189.
39. Haglund MM, Ojemann GA, Blasdel GG. Optical imaging of bipolar cortical stimulation. *J Neurosurg*. 1993;78(5):785–793.
40. Winkler AM, Ridgway GR, Webster MA, Smith SM, Nichols TE. Permutation inference for the general linear model. *Neuroimage*. 2014;92:381–397.
41. Yeh FC, Panesar S, Fernandes D, et al. Population-averaged atlas of the macroscale human structural connectome and its network topology. *Neuroimage*. 2018;178:57–68.
42. Mayka MA, Corcos DM, Leurgans SE, Vaillancourt DE. Three-dimensional locations and boundaries of motor and premotor cortices as defined by functional brain imaging: A meta-analysis. *Neuroimage*. 2006;31(4):1453–1474.
43. Archer DB, Vaillancourt DE, Coombes SA. A template and probabilistic atlas of the human sensorimotor tracts using diffusion MRI. *Cereb Cortex*. 2018;28(5):1685–1699.
44. Chen DQ, Dell'Acqua F, Rokem A et al. Diffusion weighted image co-registration: Investigation of best practices. *bioRxiv*. [Preprint] doi:10.1101/864108
45. Dell'Acqua F, Simmons A, Williams SCR, Catani M. Can spherical deconvolution provide more information than fiber orientations? Hindrance modulated orientational anisotropy, a true-tract specific index to characterize white matter diffusion. *Hum Brain Mapp*. 2013;34(10):2464–2483.
46. DeMarco AT, Turkeltaub PE. A multivariate lesion symptom mapping toolbox and examination of lesion-volume biases and correction methods in lesion-symptom mapping. *Hum Brain Mapp*. 2018;39(11):4169–4182.
47. De Renzi E, Motti F, Nichelli P. Imitating gestures: A quantitative approach to ideomotor apraxia. *Arch Neurol*. 1980;37(1):6–10.
48. Zhang Y, Kimberg DY, Coslett HB, Schwartz MF, Wang Z. Multivariate lesion-symptom mapping using support vector regression. *Hum Brain Mapp*. 2014;35(12):5861–5876.
49. Tzourio-Mazoyer N, Landeau B, Papathanassiou D, et al. Automated anatomical labeling of activations in SPM using a macroscopic anatomical parcellation of the MNI MRI single-subject brain. *Neuroimage*. 2002;15(1):273–289.
50. Kamada K, Todo T, Ota T, et al. The motor-evoked potential threshold evaluated by tractography and electrical stimulation: Clinical article. *J Neurosurg*. 2009;111(4):785–795.
51. Nossek E, Korn A, Shahar T, et al. Intraoperative mapping and monitoring of the corticospinal tracts with neurophysiological assessment and 3-dimensional ultrasonography-based navigation. Clinical article. *J Neurosurg*. 2011;114(3):738–746.
52. Ohue S, Kohno S, Inoue A, et al. Accuracy of diffusion tensor magnetic resonance imaging-based tractography for surgery of gliomas near the pyramidal TractA significant correlation between subcortical electrical stimulation and postoperative tractography. *Neurosurgery*. 2012;70(2):283–294.
53. Prabhu SS, Gasco J, Tummala S, Weinberg JS, Rao G. Intraoperative magnetic resonance imaging-guided tractography with integrated monopolar subcortical functional mapping for resection of brain tumors: Clinical article. *J Neurosurg*. 2011; 114(3):719–726.
54. Mohan UR, Watrous AJ, Miller JF, et al. The effects of direct brain stimulation in humans depend on frequency, amplitude, and white-matter proximity. *Brain Stimul*. 2020;13(5):1183–1195.
55. Liu J, Wang C, Qin W, et al. Corticospinal fibers with different origins impact motor outcome and brain after subcortical stroke. *Stroke*. 2020;51(7):2170–2178.
56. Newton JM, Ward NS, Parker GJM, et al. Non-invasive mapping of corticofugal fibres from multiple motor areas—relevance to stroke recovery. *Brain*. 2006;129(Pt 7):1844–1858.
57. Potter-Baker KA, Varnerin NM, Cunningham DA, et al. Influence of corticospinal tracts from higher order motor cortices on recruitment curve properties in stroke. *Front Neurosci*. 2016;10:79.
58. McNeal DW, Darling WG, Ge J, et al. Selective long-term reorganization of the corticospinal projection from the supplementary motor cortex following recovery from lateral motor cortex injury. *J Comp Neurol*. 2010;518(5):586–621.
59. Morecraft RJ, Ge J, Stilwell-Morecraft KS, Rotella DL, Pizzimenti MA, Darling WG. Terminal organization of the corticospinal projection from the lateral premotor cortex to the cervical enlargement (C5–T1) in rhesus monkey. *J Comp Neurol*. 2019; 527(16):2761–2789.
60. Caggiano V, Sur M, Bizzi E. Rostro-caudal inhibition of hindlimb movements in the spinal cord of mice. *PLoS One*. 2014;9(6):e100865.
61. Kitsikis A. The suppression of arm movements in monkeys: Threshold variations of caudate nucleus stimulation. *Brain Res*. 1968;10(3):460–462.
62. Kitsikis A, Rougeul A. The effect of caudate stimulation on conditioned motor behavior in monkeys. *Physiol Behav*. 1968;3(6): 831–837.
63. Jahanshahi M, Obeso I, Rothwell JC, Obeso JA. A fronto-striato-subthalamic-pallidal network for goal-directed and habitual inhibition. *Nat Rev Neurosci*. 2015;16(12):719–732.
64. Aron AR, Herz DM, Brown P, Forstmann BU, Zaghoul K. Frontosubthalamic circuits for control of action and cognition. *J Neurosci*. 2016;36(45):11489–11495.
65. Schucht P, Moritz-Gasser S, Herbet G, Raabe A, Duffau H. Subcortical electrostimulation to identify network subserving motor control. *Hum Brain Mapp*. 2013;34(11):3023–3030.
66. Kinoshita M, de Champfleury NM, Deverduin J, Moritz-Gasser S, Herbet G, Duffau H. Role of fronto-striatal tract and frontal aslant tract in movement and speech: An axonal mapping study. *Brain Struct Funct*. 2015;220(6):3399–3412.
67. Côté SL, Hamadjida A, Quessy S, Dancause N. Contrasting modulatory effects from the dorsal and ventral premotor cortex on primary motor cortex outputs. *J Neurosci*. 2017;37(24):5960–5973.

68. Rosett J. *Intercortical Systems of the Human Cerebrum*. Columbia University Press; 1933. doi:10.7312/rose91600
69. Catani M, Dell'acqua F, Vergani F, et al. Short frontal lobe connections of the human brain. *Cortex*. 2012;48(2):273–291.
70. Guevara M, Román C, Houenou J, et al. Reproducibility of superficial white matter tracts using diffusion-weighted imaging tractography. *Neuroimage*. 2017;147:703–725.
71. Kirilina E, Helbling S, Morawski M, et al. Superficial white matter imaging: Contrast mechanisms and whole-brain in vivo mapping. *Sci Adv*. 2020;6(41):eaaz9281.
72. Simone L, Viganò L, Fornia L, et al. Distinct functional and structural connectivity of the human hand-knob supported by intra-operative findings. *J Neurosci*. 2021;41(19):4223–4233.
73. Howells H, Puglisi G, Leonetti A, et al. The role of left fronto-parietal tracts in hand selection: Evidence from neurosurgery. *Cortex*. 2020;128:297–311.
74. Borra E, Luppino G. Large-scale temporo-parieto-frontal networks for motor and cognitive motor functions in the primate brain. *Cortex*. 2019;118:19–37.
75. Sani I, McPherson BC, Stemmann H, Pestilli F, Freiwald WA. Functionally defined white matter of the macaque monkey brain reveals a dorso-ventral attention network. *Elife*. 2019;8:e40520.
76. Ferbert A, Priori A, Rothwell JC, Day BL, Colebatch JG, Marsden CD. Interhemispheric inhibition of the human motor cortex. *J Physiol*. 1992;453(1):525–546.
77. Daskalakis ZJ, Christensen BK, Fitzgerald PB, Roshan L, Chen R. The mechanisms of interhemispheric inhibition in the human motor cortex. *J Physiol*. 2002;543(Pt 1):317–326.
78. Meyer B-U, Röricht S, Woiciechowsky C. Topography of fibers in the human corpus callosum mediating interhemispheric inhibition between the motor cortices. *Ann Neurol*. 1998;43(3):360–369.
79. Makris N, Kennedy DN, McInerney S, et al. Segmentation of sub-components within the superior longitudinal fascicle in humans: A quantitative, in vivo, DT-MRI study. *Cereb Cortex*. 2005;15(6):854–869.
80. Thiebaut de Schotten M, Dell'Acqua F, Forkel SJ, et al. A lateralized brain network for visuospatial attention. *Nat Neurosci*. 2011;14(10):1245–1246.
81. Kleist K. *Gehirmpathologie*. 1934. Accessed 5 May 2021. <https://psycnet.apa.org/record/1934-19904-001>.
82. Leiguarda RC, Marsden CD. Limb apraxias. Higher-order disorders of sensorimotor integration. *Brain*. 2000;123(5):860–879.
83. Fogassi L, Gallese V, Buccino G, Craighero L, Fadiga L, Rizzolatti G. Cortical mechanism for the visual guidance of hand grasping movements in the monkey: A reversible inactivation study. *Brain*. 2001;124(Pt 3):571–586.
84. Davare M, Andres M, Cosnard G, Thonnard J-L, Olivier E. Dissociating the role of ventral and dorsal premotor cortex in precision grasping. *J Neurosci*. 2006;26(8):2260–2268.
85. Naito E, Roland PE, Grefkes C, et al. Dominance of the right hemisphere and role of area 2 in human kinesthesia. 2005;93(2):1020–1034.
86. Naito E, Ehrsson HH. Somatic sensation of hand-object interactive movement is associated with activity in the left inferior parietal cortex. *J Neurosci*. 2006;26(14):3783–3790.
87. Gerbella M, Borra E, Mangiaracina C, Rozzi S, Luppino G. Corticostriate projections from areas of the “lateral grasping network”: Evidence for multiple hand-related input channels. *Cereb Cortex*. 2016;26(7):3096–3115.
88. Catani M, Mesulam MM, Jakobsen E, et al. A novel frontal pathway underlies verbal fluency in primary progressive aphasia. *Brain*. 2013;136(Pt 8):2619–2628.
89. Rizio AA, Diaz MT. Language, aging, and cognition: Frontal aslant tract and superior longitudinal fasciculus contribute toward working memory performance in older adults. *Neuroreport*. 2016;27(9):689–693.
90. Budisavljevic S, Dell'Acqua F, Djordjilovic V, Miotto D, Motta R, Castiello U. The role of the frontal aslant tract and premotor connections in visually guided hand movements. *Neuroimage*. 2017;146:419–428.
91. Krainik A, Lehericy S, Duffau H, et al. Role of the supplementary motor area in motor deficit following medial frontal lobe surgery. *Neurology*. 2001;57(5):871–878.
92. Schulz R, Braass H, Liuzzi G, et al. White matter integrity of premotor-motor connections is associated with motor output in chronic stroke patients. *NeuroImage Clin*. 2015;7:82–86.
93. Bocconi L, Meyer S, D'cruz N, et al. Premotor dorsal white matter integrity for the prediction of upper limb motor impairment after stroke. *Sci Rep*. 2019;9(1):1–9.
94. Rizzi M, Sartori I, Del Vecchio M, et al. Tracing in vivo the dorsal loop of the optic radiation: convergent perspectives from tractography and electrophysiology compared to a neuroanatomical ground truth. *Res Sq*. [Preprint]. doi:10.21203/RS.3.RS-589114/V1